# Supporting Information

## A highly stable $Mn^{II}$ phosphonate as highly efficient catalyst for $CO_2$ fixation under ambient conditions

Yang Yang,[a] Chao-Ying Gao,[ab] Hong-Rui Tian,[b] Jing Ai,[b] Xue Min[b] and Zhong-Ming Sun*[b]

[a] Inner Mongolia Key Lab of Chemistry of Natural Products and Synthesis of Functional Molecules, College of Chemistry and Chemical Engineering, Inner Mongolia University for the Nationalities (IMUN), Tongliao 028000, People's Republic of China

[b] State Key Laboratory of Rare Earth Resource Utilization, Changchun Institute of Applied Chemistry, Chinese Academy of Sciences, 5625 Renmin Street, Changchun, Jilin 130022, China.

*Corresponding Authors. E-mail: szm@ciac.ac.cn

### Supplementary Index

Contents

## S1. Materials and Methods

### 1.1 General information

Materials and Instrument

All materials are commercially available and were used without further purification except for pyridin-4-yl-phosphonic acid ($H_2L$), which was synthesized by a modified procedure documented previously.[1]

Powder X-ray diffraction (PXRD) was carried out at 40 kV and 40 mAon a MiniFlex 600 X-ray powder diffractometer equipped with a Cu sealed tube ($\lambda$ = 1.541 78 Å) over 2$\theta$ range of 5-50$^o$ at room temperature. Thermal gravimetric analysis (TGA) was conducted on a SDT 2960 Simultaneous DSC-TGA of TA instruments with a heating rate of 10 $^o$C/min up to 900 $^o$C under an air atmosphere. Elemental analyses for C, H, and N were performed by a VarioEL analyzer. The infrared (IR) spectra (diamond) were recorded on a Nicolet 7600 FT-IR spectrometer within the 4000-500 $cm^{-1}$ region. Inductively coupled plasma (ICP) analyses were conducted on a Perkin-Elmer Optima 3300DV spectrometer. $^1$H NMR spectra were carried out in $CDCl_3$ solvent on a Bruker 400 MHz spectrometer. The chemical shift is given in dimensionless δ values and is referenced relative to TMS in $^1$H spectroscopy.

### 1.2 Synthesis of compound $[MnL(H_2O)_2]\cdot H_2O$

A mixture of $Mn(Ac)_2\cdot 4H_2O$ (0.2 mmol, 49 mg), pyridin-4-yl-phosphonic acid ($H_2L$) (0.5mmol, 80 mg) and distilled water (6 ml) was sealed in a Teflon-lined stainless steel autoclave (20 mL) under autogenous pressure and heated at 80 $^o$C oven for 3 days. After the autoclave was cooled to room temperature, light-yellow block-shaped single crystals suitable for single-crystal X-ray crystallographic analysis were harvested as synthesized. Then, the mother liquor was decanted, and the resulting crystals were dried at room temperature overnight. Yield: 46.6 mg (87 % based on $Mn^{II}$). Phase purity was confirmed by PXRD analysis. FTIR ($cm^{-1}$): 1606 (w), 1418 (w), 1130 (s), 1084 (vs), 1010 (vs), 823 (s), 682 (w), 642(w), 542 (s). Elemental analysis calca (%) for $MnC_5NPO_6H_{12}$ (Mr = 268.1): C, 22.4; N, 5.2; H, 4.5. Found: C, 22.6; N, 5.1; H, 4.8.

### 1.3 Single-Crystal X-ray Crystallography

Single-crystal X-ray diffraction (SXRD) data of compound $[MnL(H_2O)_2]\cdot H_2O$ were collected on a Bruker diffractometer using Cu K$\alpha$ radiation ($\lambda$ = 1.54178 Å) at 293 K. Data processing was accomplished with the SAINT processing program.[2] The structure was solved by the direct methods and refined by full-matrix least-squares fitting on $F^2$ using the SHELXTL crystallographic software package.[3] Non-hydrogen atoms were refined with anisotropic displacement parameters during the final cycles. All hydrogen atoms of the organic molecule were placed by geometrical considerations and were added to the structure factor calculation. The final formula of $[MnL(H_2O)_2]\cdot H_2O$ was determined by single-crystal X-ray diffraction, TGA and elemental analysis.
Crystallographic data for $[MnL(H_2O)_2]\cdot H_2O$ (1565561) has been deposited with Cambridge Crystallographic Data Centre. Data can be obtained free of charge upon request at www.ccdc.cam.ac.uk/data_request/cif. Crystal data and structure refinement is summarized in Table S1.

**1.4 Chemical stability Test**

Several batches of about 5 mg of freshly synthesized samples were added into vials containing 3 mL of aqueous solutions (pH = 2-12), pure water and various organic solvents, respectively. After immersion in those solutions for given times at room temperature or at 100 $^{o}$C, the samples were centrifuged and then dried naturally.

**1.5 ICP procedure**

Firstly, the filter liquor after catalytic reaction is incinerated at about 500 degrees in the ceramic crucible; secondly, the alkali is dissolved; thirdly, the acid is neutralized; finally, the solution is added to the instrument for analysis.

**1.6 Catalysis**

In a typical reaction, the catalytic reaction was conducted in a Schlenk tube using the epoxides (20 mmol, 1850 mg for epichlorohydrin, 2733 mg for epibromohydrin, 2400 mg for styrene oxide, 3000 mg for 1,2-epoxy-3-phenoxypropane, 1420 mg forglycidol, 1442 mg for epoxybutane, 2604 mg for *n*-Butyl glycidyl ether) with $CO_2$ purged at 1 atm under solvent free environment at room temperature catalyzed by the activated sample (0.02mmol, 4 mg) and co-catalyst of tetrabutylammonium bromide (TBAB, 0.6g) for different intervals. The loading of the catalyst is a 0.1%ratio based on the epoxide. After given reaction time, a small aliquot of the supernatant reaction mixtures was dissolved in 0.6 mL of $CDCl_3$. The obtained solution was filtered through a syringe filter (PTFE) to be analyzed by $^{1}$H NMR for calculating the conversion of the epoxide. For the recycle experiment, the catalyst was separated by centrifugation for 5 min after the reaction, and the supernatant was collected. The residual solid was washed with dichloromethane and centrifuged three times before being applied the next catalytic conditions.

**1.7 Cycloaddition of $CO_2$ to epoxides**

The conversion was calculated from $^{1}$H NMR according to the following equation.

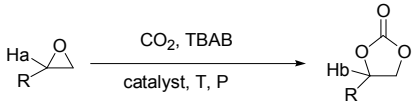


$$\text{conversion} = \frac{^{1}Hb}{(^{1}Ha + ^{1}Hb)}$$

## S2 Supplementary tables and figures

**Table S1** Crystallographic data

| | |
|---|---|
| Formula | $MnC_5NPO_5H_{10}$ |
| $F_w$ | 250.05 |
| Crystal system | trigonal |
| Space group | *R-3* |
| a, Å | 28.9848(19) |
| b, Å | 28.9848(19) |
| c, Å | 5.5266(7) |
| V, Å$^3$ | 4021.0(7) |
| Z | 36 |
| $D_c$, mg/mm$^3$ | 1.933 |
| $\mu$, mm$^{-1}$ | 1.658 |
| reflection collected | 8292 |
| GOF on $F^2$ | 1.069 |
| $R_1/wR_2$ ($I > 2\sigma(I)$) | 0.0504/ 0.1270 |
| $R_1/wR_2$ (all data) | 0.0601/0.1321 |

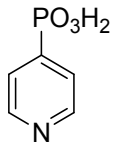


**Scheme S1**pyridin-4-yl-phosphonic acid ($H_2L$) as a ligand in this work.

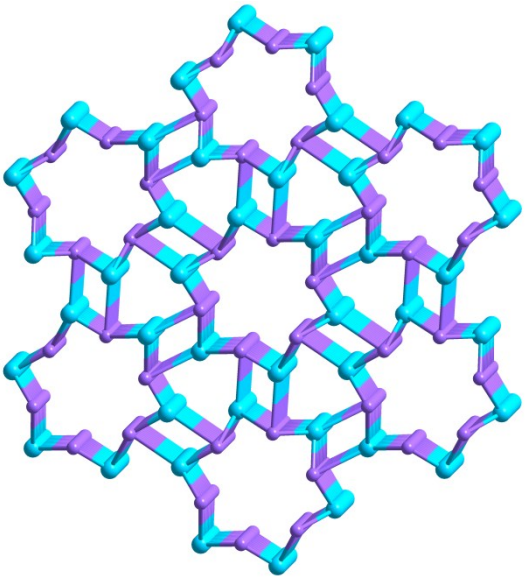

**Figure S1** Simplified 4,4-connected *ato* net of the compound.

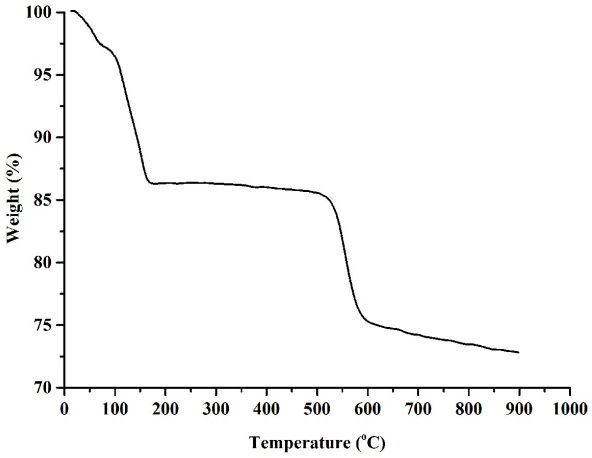


**Figure S2** Thermogravimetric analysis data for $[MnL(H_2O)_2]\cdot H_2O$.

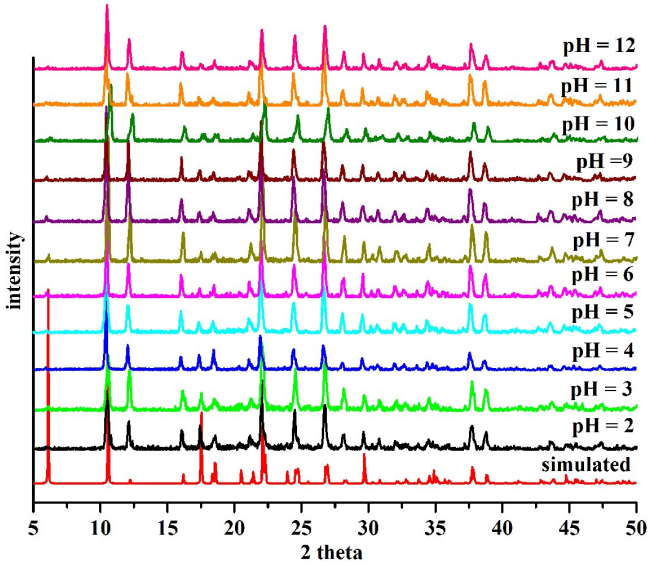


**Figure S3** PXRD patterns of $[MnL(H_2O)_2]\cdot H_2O$ upon the treatment using aqueous solution with a wide range of pH values (2 - 12).

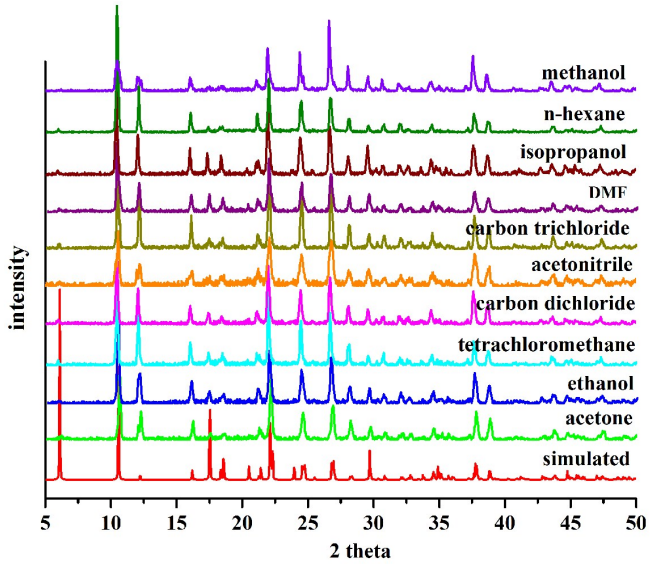


**Figure S4** PXRD patterns of $[MnL(H_2O)_2]\cdot H_2O$ upon the treatment withvariousorganic solvents.

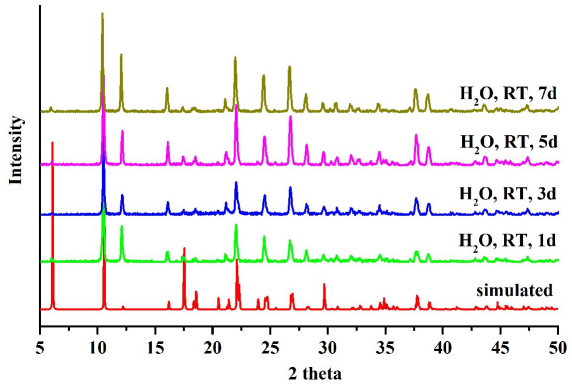


**Figure S5** PXRD patterns of $[MnL(H_2O)_2]\cdot H_2O$ upon the treatment with water.

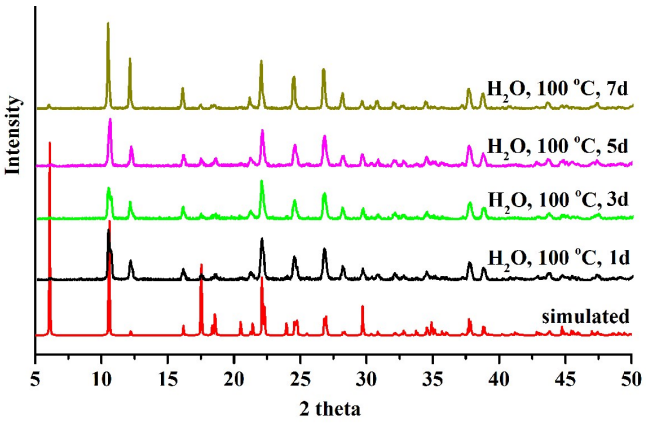


**Figure S6** PXRD patterns of $[MnL(H_2O)_2]\cdot H_2O$ upon the treatment with boiling water.

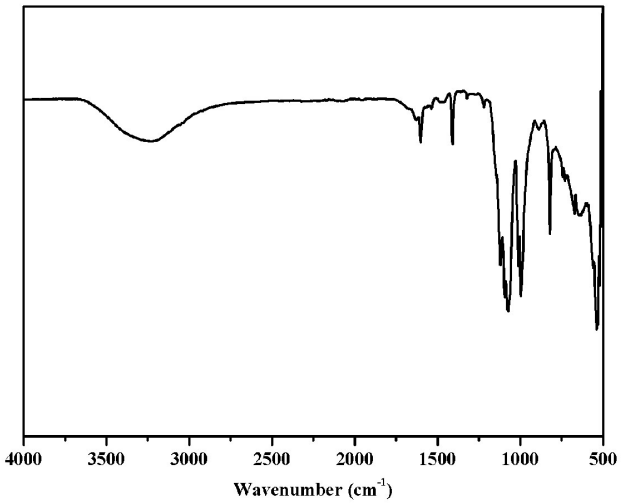


**Figure S7** Infrared spectra of the compound.

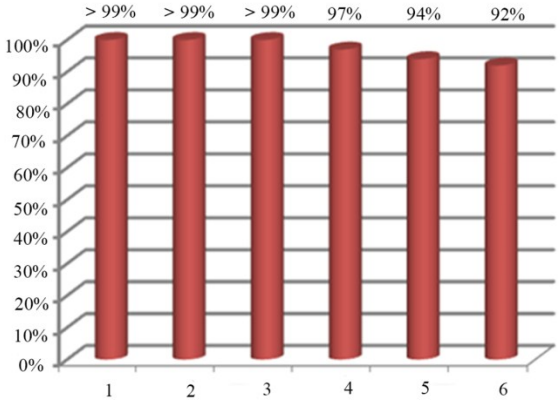


**Figure S8** Histogram of recyclibility study (six cycles) for catalytic acitivities of the catalyst in coupling of glycidol with $CO_2$.

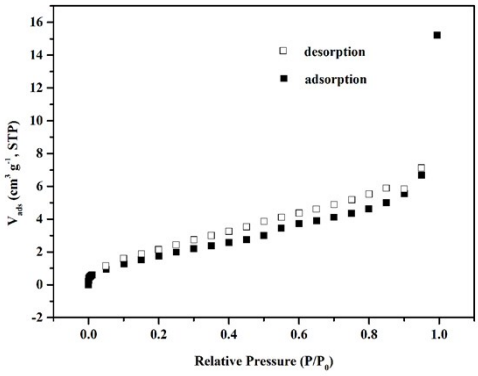


**Figure S9** The $N_2$ sorption isotherm at 77K.

The very low $N_2$ adsorption capacity may be relevant to activated diffusion effects,[22] as well as the little effective free volume of the desolvated framework, which is 15.6% (631.5 Å$^3$ out of the 4021 Å$^3$ unit cell volume) calculated by PLATON analysis.

Therefore, its porous structure was characterized using $CO_2$ adsorption at 273K (see Figure S10).

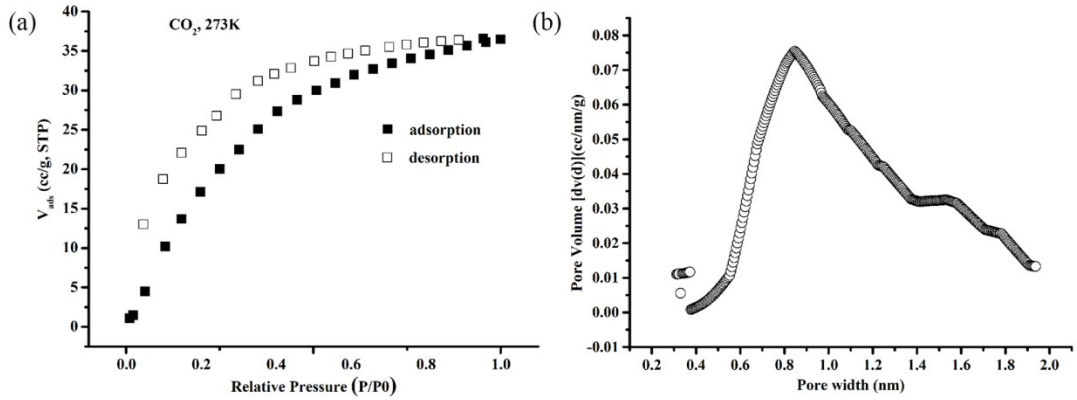


**Figure S10** (a) $CO_2$ sorption isotherms. STP = standard temperature and pressure. (b) The pore size distribution calculated using the HK method.

The pore diameter is around 0.82 nm, which is consistent with that observed in the single-crystal structure.

Activation of the $Mn^{II}$ phosphonate (evacuation at 473K for 12 h) afforded Brunauer-Emmett-Teller (BET) apparent surface area of 140.4 m$^2$ g$^{-1}$ from $CO_2$ adsorption isortherms at 273K.

**Table S2** Comparison of chemical stability conditions of selected stable MOFs.

| MOFs | Metals | Ligands | Stable conditions | Ref. |
|---|---|---|---|---|
| **PCN-57** | Zr | 2',3',5',6'-tetramethylterphenyl-4,4''-dicarboxylic acid | pH = 2-11 solutions for 2days | 4 |
| **PCN-225** | Zr | tetrakis (4-carboxyphenyl)porphyrin | Boiling water or pH = 1-11 solutions for 12h | 5 |
| **PCN-777** | Zr | 4,4',4''-s-triazine-2,4,6-triyl-tribenzoic acid | pH = 3-11 solutions for 12h | 6 |
| **$Ni_3(BTP)_2$** | Ni | 1,3,5-tris(1H-pyrazol-4-yl)benzene | Boiling aqueous solutions of pH = 2-14 for 2 weeks. | 7 |
| **PCN-250($Fe_2Co$)** | Fe; Co | 3,3',5,5'-Azobenzenetetracarboxylic | pH = 1-11 solutions for 24h. | 8 |
| **PCN-600** | Fe | tetrakis (4-carboxyphenyl)porphyrin | pH = 2-11 solutions for 24h. | 9 |
| **LaBTB** | La | 1,3,5-tris (4-carboxyphenyl) benzene | pH = 2 solution (60 $^oC$) or pH = 14 solution (60 $^oC$ or 100 $^oC$) for 3 days. | 10 |
| **$Eu_2$(D-cam)$(Himdc)_2$** | Eu | D-camphoric acid; 4,5-imidazole dicarboxylic | pH = 2-13 solutions for 2 weeks. | 11 |
| **$Cd_3(L)(bipy)_2$** | Cd | hexa[4-(carboxyphenyl)oxamethyl]-3-oxapentane | pH = 2-13 solutions for 24 h; water for 7 days. | 12 |
| **$[MnL(H_2O)_2]\cdot H_2O$** | Mn | pyridin-4-yl-phosphonic acid | pH = 2-12 solution for 24 h; boling water for 7 days; 400 $^oC$ | **This work** |

**Table S3** The $Mn^{II}$ phosphonate catalyzed coupling of epoxides with $CO_2$. Reaction conditions: epoxide (20 mmol), catalyst (0.02mmol, 0.1% based on the epoxide) and TBAB (0.6 g) under carbon dioxide (1 atm) at room temperature. The conversion was determined by $^1H$ NMR analysis.

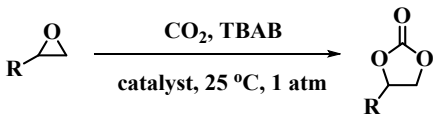


| Entry | Substrates | Time (h) | Conversion (%) |
|---|---|---|---|
| 1 | 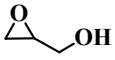 | 12 | 56.5 |
| | | 24 | 77.5 |
| | | 36 | >99 |
| 2 | 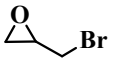 | 12 | 62.1 |
| | | 24 | 74.1 |
| | | 36 | 89.3 |
| 3 | 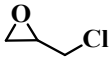 | 12 | 49.8 |
| | | 24 | 65.8 |
| | | 36 | 76.9 |
| 4 | 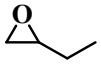 | 12 | 21.3 |
| | | 24 | 31.4 |
| | | 36 | 49.3 |
| 5 | 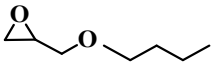 | 12 | 25.8 |
| | | 24 | 43.3 |
| | | 36 | 52.6 |
| 6 | 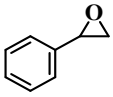 | 48 | 4.4 |
| 7 | 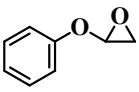 | 48 | 6.4 |

**Table S4** Comparison with different MOF catalysts in the cycloaddition reaction of $CO_2$ and the same epoxies under similar conditions.

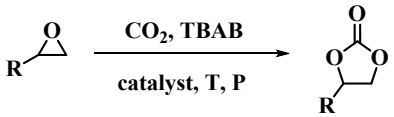


| Substrate | Catalyst | T (°C) | P (MPa) | T (h) | TON | TOF ($h^{-1}$) | Ref. |
|---|---|---|---|---|---|---|---|
|  | 1·Gd | 60 | 0.1 | 12 | 12.9 | 1.1 | 13 |
| | MOF-5 | 35 | 0.1 | 12 | 22.3 | 2.0 | 14 |
| | $\{[Eu(BTB)(phen)]\cdot 4.5DMF\cdot 2H_2O\}_n$ | 70 | 0.1 | 12 | 24.7 | 2.1 | 15 |
| | FJI-H7(Cu) | 25 | 0.1 | 60 | 332.5 | 5.5 | 16 |
| | CHB (M) | 100 | 1.2 | 6 | 44.6 | 7.0 | 17 |
| | MMPF-18 | 70 | 0.1 | 48 | 396.0 | 8.3 | 18 |
| | $[Cu_4(L_1)]_n$ | 25 | 0.1 | 48 | 425.0 | 8.9 | 19 |
| | $[MnL(H_2O)_2]\cdot H_2O$ | 25 | 0.1 | 36 | 769.0 | 21.4 | This work |
| 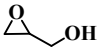 | $\{[Eu(BTB)(phen)]\cdot 4.5DMF\cdot 2H_2O\}_n$ | 70 | 0.1 | 12 | 19.6 | 1.6 | 15 |
| | $[MnL(H_2O)_2]\cdot H_2O$ | 25 | 0.1 | 36 | 1000 | 27.8 | This work |
| 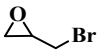 | $[Cu_4(L_1)]_n$ | 25 | 0.1 | 48 | 440.0 | 9.2 | 19 |
| | $[MnL(H_2O)_2]\cdot H_2O$ | 25 | 0.1 | 36 | 893.0 | 24.8 | This work |
|  | MMPF-18 | 25 | 0.1 | 48 | 356.0 | 8 | 18 |
| | $[Cu_4(L_1)]_n$ | 25 | 0.1 | 48 | 415.0 | 8.6 | 19 |
| | MMPF-9 | 25 | 0.1 | 48 | 642.4 | 13.4 | 20 |
| | MMCF-2 | 25 | 0.1 | 48 | 708.0 | 14.8 | 21 |
| | $[MnL(H_2O)_2]\cdot H_2O$ | 25 | 0.1 | 36 | 493.0 | 13.7 | This work |
| 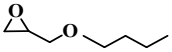 | MMPF-9 | 25 | 0.1 | 48 | 244.0 | 5.1 | 20 |
| | MMCF-2 | 25 | 0.1 | 48 | 336.8 | 7.0 | 21 |
| | $[MnL(H_2O)_2]\cdot H_2O$ | 25 | 0.1 | 36 | 526.0 | 14.6 | **This work** |

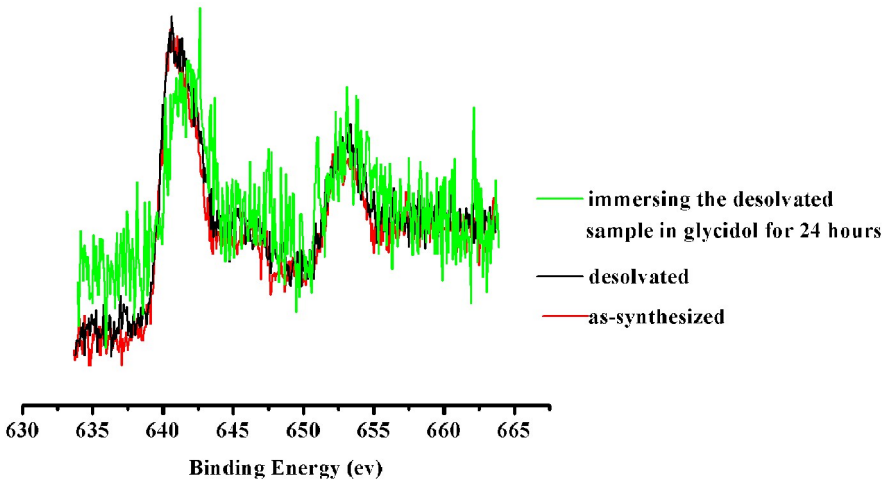


**Figure S11** X-ray photoelectron spectroscopy (XPS) Mn 2p core-level spectra of the as-synthesized and different treated samples.

The variation of major peak positions in core-level spectra of Mn 2p is discernible; the shift to the higher binding energy ascribes the electron dissociation of the Mn atoms, suggesting that there is some coordination between Mn(II) and epoxide.

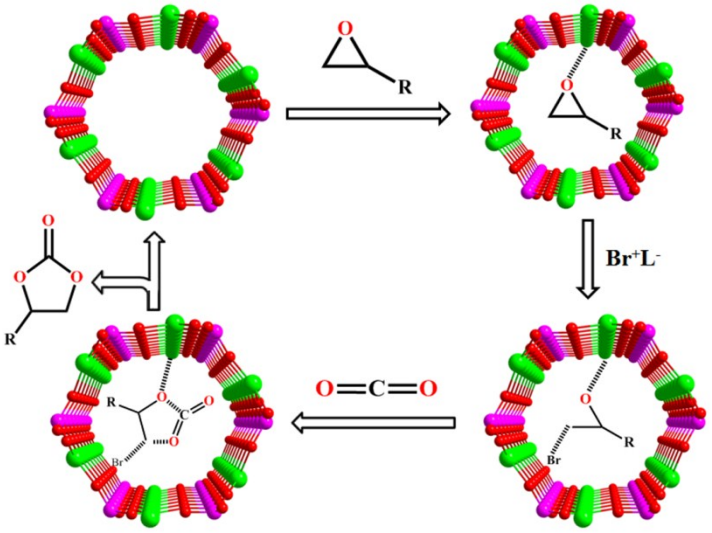


**Scheme S2** The schematic representation of the tentatively proposed catalytic mechanism for the cycloaddition of epoxides and $CO_2$ into cycliccarbonates in this work ($L^+$ = tetra-n-butylammonium). Mn: green; O: red; P: pink; C: black.

## S3 The NMR spectrums

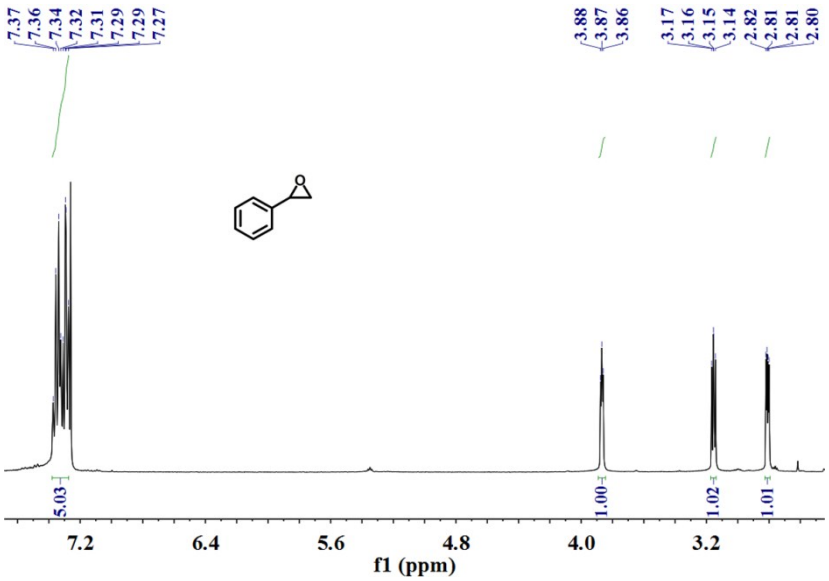


**Figure S12** $^{1}$H NMR spectra of styrene oxide (400 MHz, $CDCl_3$): δ = 7.27 – 7.37 (m, 5H, Ar-H), 3.87 (t, J=4.0 Hz, 1H, O-CH*), 3.16 (q, J=4.0 Hz, 1H, O-$CH_2$), 2.81 (q, J = 4.0 Hz, 1H, O-$CH_2$).

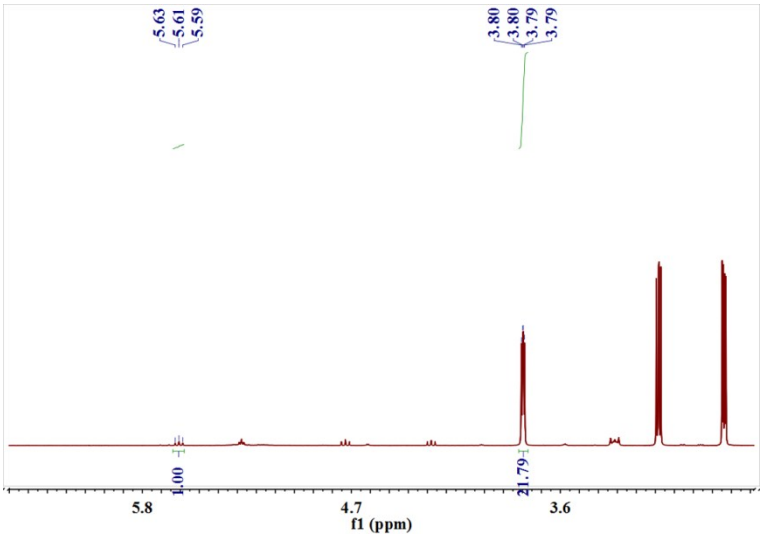


**Figure S13** $^{1}$H NMR spectra of the cycloaddition product of styrene oxide and $CO_2$ for 48 h (400 MHz, $CDCl_3$) : δ = 5.60 (t, J = 8.0 Hz, 1H, COO-CH* of product), , 3.79-3.80 (t, J = 8.0 Hz, 2.20H, O-CH* of raw material).

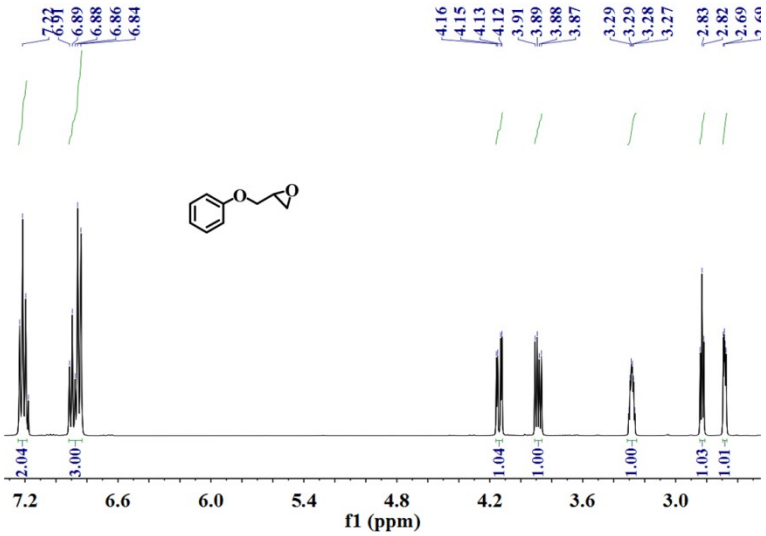


**Figure S14** $^{1}$H NMR spectra of 1,2-epoxy-3-phenoxypropane (400 MHz, $CDCl_3$) : δ = 7.18 – 7.23 (m, 2H, Ar-H), 6.84 – 6.91 (m, 3H, Ar-H), 4.14 (q, J = 4.0 Hz, 1H, ArO-$CH_2$), 3.88 (q, J = 4.0 Hz, 1H, ArO-$CH_2$), 3.26 – 3.30 (m, 1H,O-CH*), 2.83 (t, J = 4.0 Hz, 1H,O-$CH_2$), 2.68 (q, J = 4.00 Hz, 1H,O-$CH_2$).

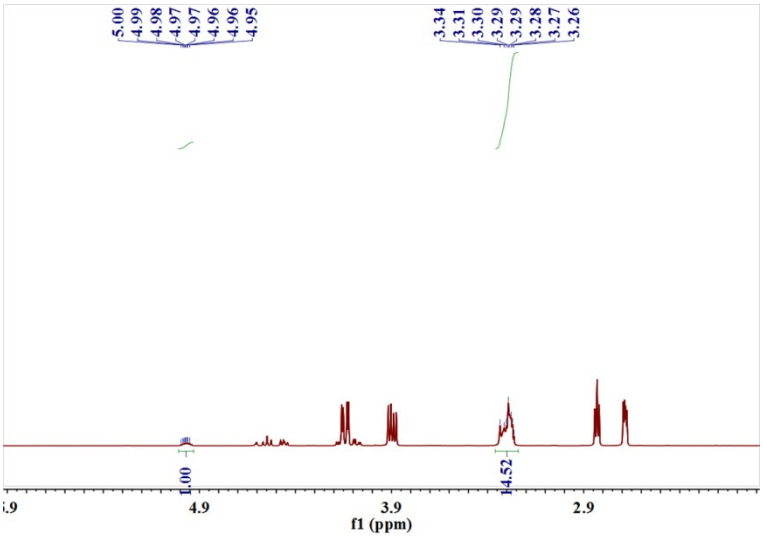


**Figure S15** $^{1}$H NMR of the cycloaddition product of 1,2-epoxy-3-phenoxypropane and $CO_2$ for 48 h (400 MHz, $CDCl_3$): δ = 4.95 – 5.00 (m, 1H, COO-CH* of product), 4.55 (t, J = 8.0 Hz, 1H, COO-$CH_2$), 3.26 – 3.34 (m, 0.46H, O-CH* of raw material).

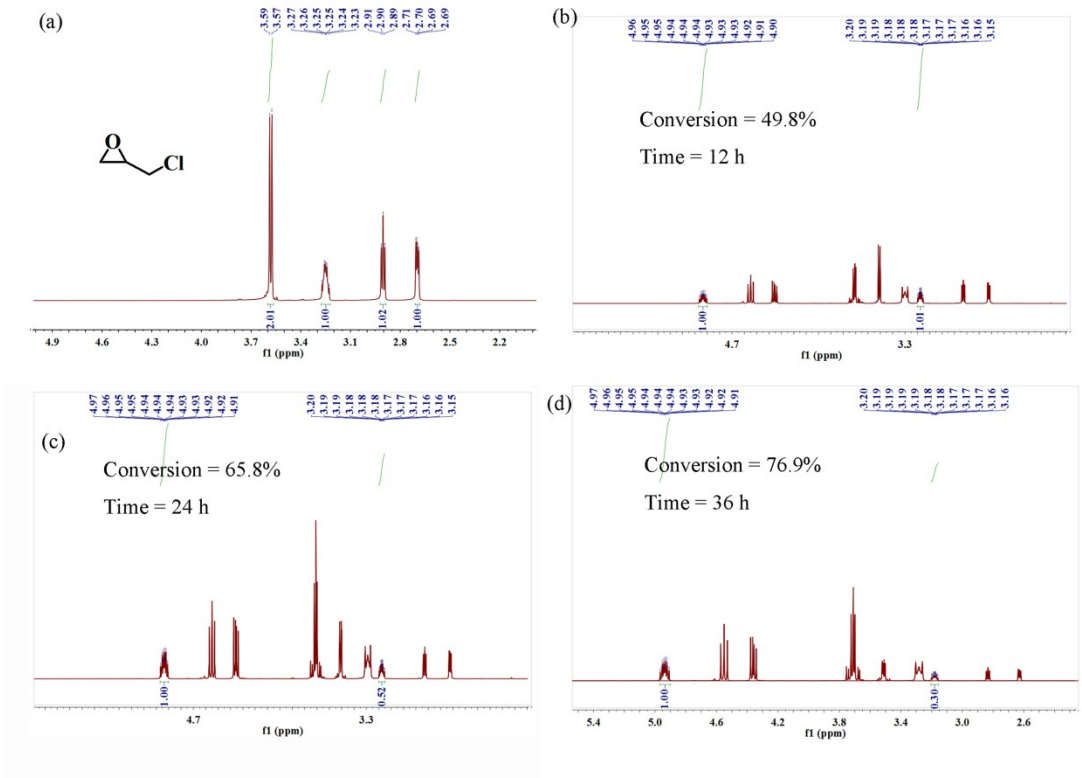


**Figure S16** (a) $^{1}H$ NMR spectra of epichlorohydrin (400 MHz, $CDCl_3$): δ = 3.58 (d, J = 8.0 Hz, 2H, Cl-$CH_2$), 3.23 – 3.27 (m, 1H, O-CH*), 2.90 (t, J = 4.0 Hz, 1H, O-$CH_2$), 2.70 (q, J = 4.0 Hz, 1H, O-$CH_2$).

(b-d) $^{1}H$ NMR spectra of the cycloaddition product of epichlorohydrin and $CO_2$ catalyzed for 12 h, 24 h 36 h, respectively (400 MHz, $CDCl_3$) : δ = 4.90 – 4.97 (m, 1H, COO-CH* of product), 3.15 – 3.20 (m, 1H, O-CH* of raw material).

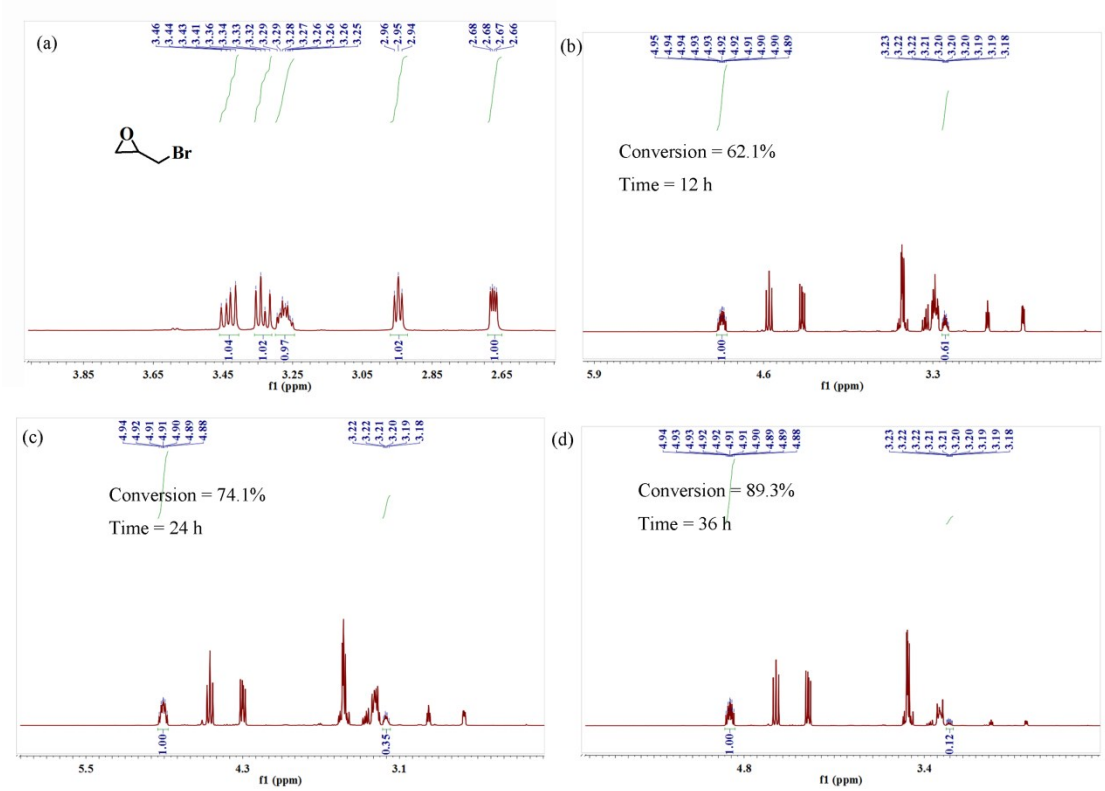


**Figure S17** (a) $^{1}$H NMR spectra of epibromohydrin (400 MHz, $CDCl_3$): δ = 3.42 (q, J = 8.0 Hz, 1H, Br-$CH_2$), 3.33 (q, J = 8.0 Hz, 1H, Br-$CH_2$), 3.25 – 3.29 (m, 1H, O-CH*), 2.95 (t, J = 4.0 Hz, 1H, O-$CH_2$), 2.67 (q, J = 4.0 Hz, 1H, O-$CH_2$).

(b-d) $^{1}$H NMR spectra of the cycloaddition product of epibromohydrin and $CO_2$ for 12 h, 24 h, 36 h, respectively (400 MHz, $CDCl_3$) : δ = 4.88 – 4.95 (m, 1H, COO-CH* of product), 3.18–3.23 (m, 1H, O-CH* of raw material).

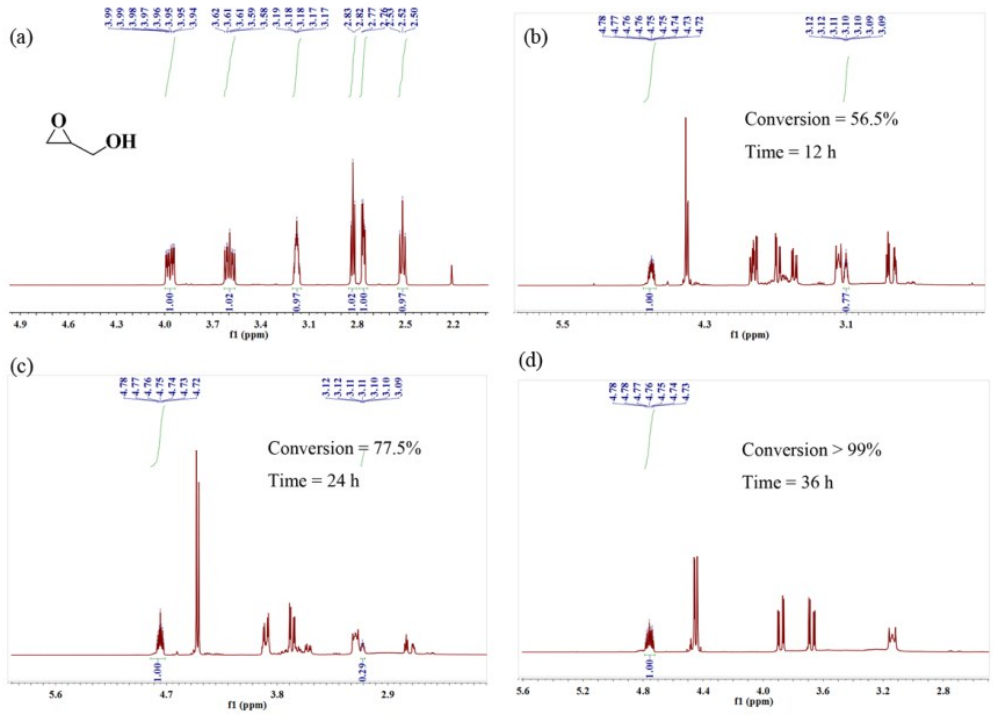


**Figure S18** (a) $^{1}$H NMR spectra of glycidol (400 MHz, $CDCl_3$): δ = 3.94 – 3.99 (m, 1H, HO-$CH_2$), 3.56 – 3.62 (m, 1H, $HOCH_2$),3.16 – 3.19 (m, 1H, O-CH*), 2.83 (t, J = 4.0 Hz, 1H, O-$CH_2$), 2.76 (q, J = 4.0 Hz, 1H, O-$CH_2$), 2.52 (t, J = 4.0 Hz,1H, -OH).

(b-d) $^{1}$H NMR spectra of the cycloaddition product of glycidol and $CO_2$ for 12 h, 24 h, 36 h, respectively (400 MHz, $CDCl_3$) : δ = 4.72 – 4.78 (m, 1H, COO-CH* of product), 3.09–3.12(m, 1H, O-CH* of raw material).

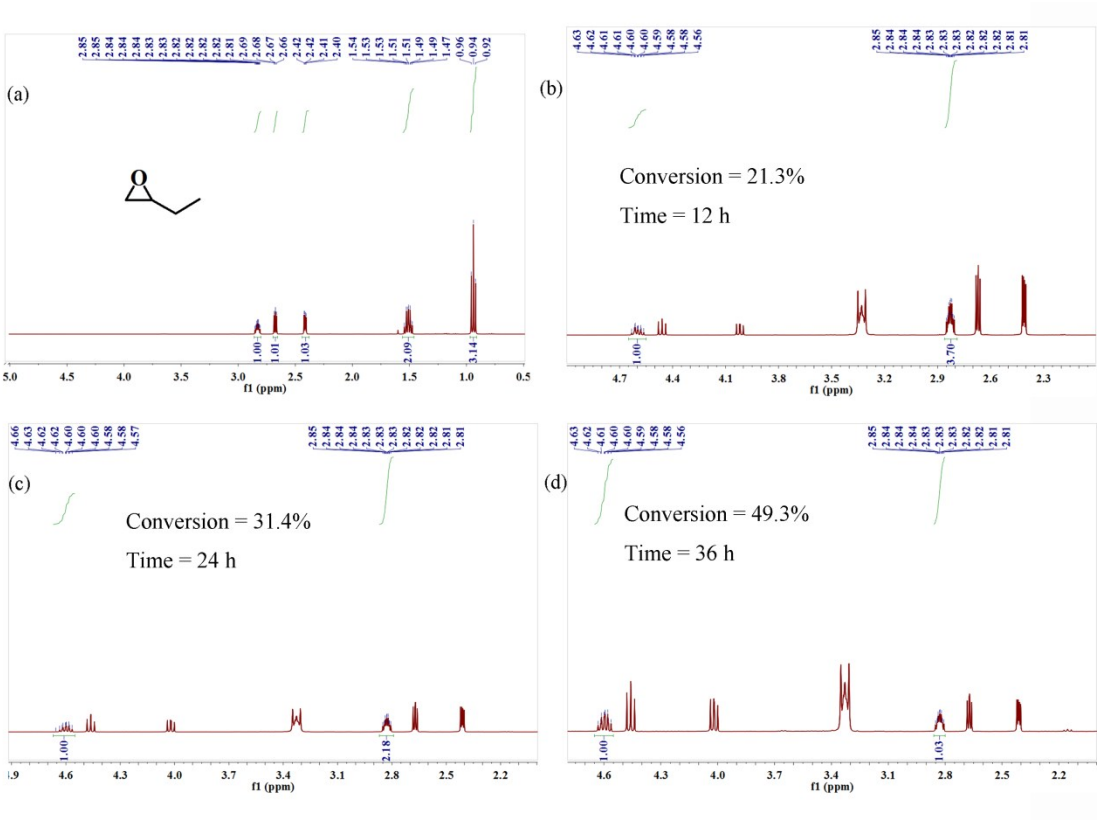


**Figure S19** (a) $^{1}$H NMR spectra of epoxybutane (400 MHz, $CDCl_3$): δ = 2.83 (m, 1H, O-CH*), 2.67 (t, J = 5.0, 4.0 Hz, 1H, O-$CH_2$), 2.41 (m, 1H, O-$CH_2$), 1.51 (m, 2H, -$CH_2$), 0.94 (t, J = 7.5 Hz, 3H, -$CH_3$).

(b-d) $^{1}$H NMR spectra of the cycloaddition product of epoxybutane and $CO_2$ for 12 h, 24 h, 36 h, respectively (400 MHz, $CDCl_3$) : δ = 4.56 – 4.93 (m, 1H, COO-CH* of product), 2.81-2.85 (m, 1H, O-CH* of raw material).

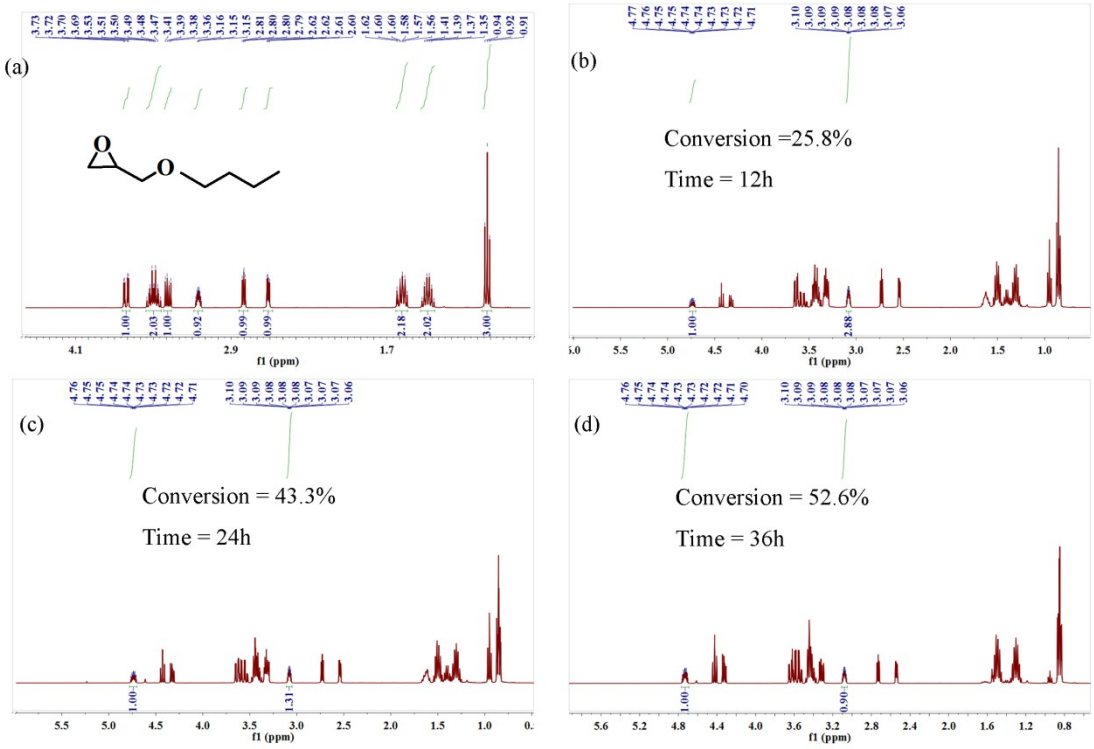


**Figure S20** (a) $^1$H NMR spectra of *n*-Butyl glycidyl ether (400 MHz, $CDCl_3$): δ = 3.73-3.69 (dd, J = 11.5, 3.1 Hz, 1H, O-$CH_2$-cycle), 3.55-3.44 (m, 2H, O-$CH_2$-chain), 3.41-3.36 (m, 1H, O-$CH_2$-cycle), 3.17-3.13 (t, J = 5.8, 4.1, 2.9 Hz, 1H, O-CH*-cycle), 2.81-2.79 (dd, J = 5.0, 4.2 Hz, 1H, O-$CH_2$-chain), 2.62-2.60 (dd, J = 5.0, 2.7 Hz, 1H, O-$CH_2$-chain), 1.62 – 1.54 (m, 2H, -$CH_2$-), 1.43 – 1.33 (m, 2H, -$CH_2$-), 0.94-0.91 (t, J = 7.4 Hz, 3H, -$CH_3$).

(b-d) $^1$H NMR spectra of the cycloaddition product of *n*-Butyl glycidyl ether and $CO_2$ for 12 h, 24 h, 36 h, respectively (400 MHz, $CDCl_3$) : δ = 4.76 – 4.71 (m, 1H, COO-CH* of product), 3.10-3.06 (m, 1H, O-CH* of raw material).

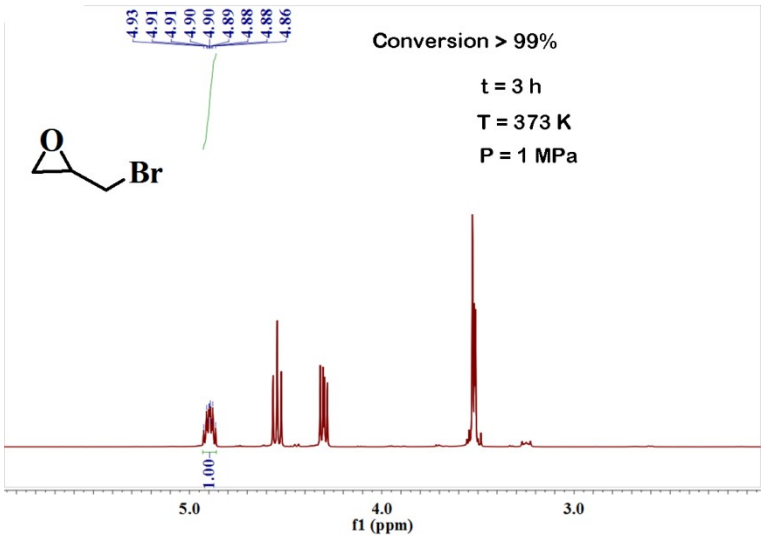


**Figure S21** $^1$H NMR spectra of the cycloaddition product of epibromohydrin and $CO_2$ for 3 h at 373 K and under 1 MPa.

## S4 References


1. (a) Patent: WO2008/10985A2, 2008; (b) D. Redmore，*J. Org. Chem*., 1976, **41**, 2149.
2. SMART and SAINT software package, Siemens Analytical X-ray Instruments Inc., Madison, WI, 1996.
3. (a) O.V. Dolomanov, L.J. Bourhis, R.J. Gildea, J. A. K. Howard and H. Puschmann, *J. Appl. Cryst.* 2009, **42**, 339; (b) G. M. Sheldrick, *ActaCryst. A*, 2008, **64**, 112; (c) G. M. Sheldrick, *ActaCryst. C*, 2015, **71**, 3.
4. H.-L. Jiang, D. Feng, T.-F. Liu, J.-R. Li and H.-C. Zhou, *J. Am. Chem. Soc.*, 2012, **134**, 14690.
5. H.-L. Jiang, D. Feng, K. Wang, Z.-Y. Gu, Z. Wei, Y.-P. Chen and H.-C. Zhou, *J. Am. Chem. Soc.*, 2013, **135**, 13934.
6. D. Feng, K. Wang, J. Su, T.-F. Liu, J. Park, Z. Wei, M. Bosch, A. Yakovenko, X. Zou and H.-C. Zhou, *Angew. Chem. Int. Ed.*, 2015, **54**, 149.
7. V. Colombo, S. Galli, H. J. Choi, G. D. Han, A. Maspero, G. Palmisano, N. Masciocchi, J. R. Long, *Chem. Sci.*, 2011, 2, 1311.
8. D. Feng, K. Wang, Z. Wei, Y.-P. Chen, C. M. Simon, R. K. Arvapally, R. L. Martin, M. Bosch, T.-F. Liu, S. Fordham, D. Yuan, M. A. Omary, M. Haranczyk, B. Smit and H.-C. Zhou, *Nat. Commun.*, 2015, **5**, 5723.
9. K. Wang, D. Feng, T.-F. Liu, J. Su, S. Yuan, Y.-P. Chen, M. Bosch, X. Zou and H.-C. Zhou, *J. Am. Chem. Soc.*, 2014, **136**, 13983.
10. J. Duan, M. Higuchi, S. Horike, M. L. Foo, K. P. Rao, Y. Inubushi, T. Fukushima and S. Kitagawa, *Adv. Funct. Mater*., 2013, **23**, 3525.
11. Y.-H. Han, C.-B. Tian, Q.-H. Li and S.-W. Du, *J. Mater. Chem. C*, 2014, **2**, 8065.
12. F.-Y. Yi, Y. Wang, J.-P. Li, D. Wu, Y.-Q. Lan and Z.-M. Sun, *Mater. Horiz.*, 2015, **2**, 245.
13. J. Dong, P. Cui, P.-F. Shi and B. Zhao, *J. Am. Chem. Soc., 2015,* **137** *,* 15988.
14. J. Song, Z. Zhang, S. Hu, T. Wu, T. Jiang and B. Han, *Green Chem.*, 2009, **11**, 1031.
15. H. Xu, B. Zhai, C.-S. Cao and B. Zhao, *Inorg. Chem*., 2016, **55**, 9671.
16. J. Zheng, M. Wu, F. Jiang, W. Su and M. Hong, *Chem. Sci*., 2015, **6**, 3466.
17. A. C. Kathalikkattil, D. W. Kim, J. Tharun, H. G. Soek, R. Roshan and D. W. Park, *Green Chem*. 2014, **16**, 1607.
18. W.-Y. Gao, C.-Y. Tsai, L. Wojtas, T. Thiounn, C.-C. Lin and S. Ma, *Inorg. Chem*., 2016, **55**, 7291.
19. P.-Z. Li, X.-J. Wang, J. Liu, J.S. Lim, R. Zou and Y. Zhao, *J. Am. Chem. Soc*., 2016, **138**, 2142.
20. W.-Y. Gao, L. Wojtas and S. Ma, *Chem. Commun*., 2014, **50**, 5316.
21. W.-Y. Gao, Y. Chen, Y. Niu, K. Williams, L. Cash, P. J. Perez, L. Wojtas, J. Cai, Y.-S. Chen and S. Ma, *Angew. Chem. Int. Ed*., 2014, **53**, 2615.
22. B. Chen, X. Zhao, A. Putkham, K. Hong, E. B. Lobkovsky, E. J. Hurtado, A. J. Fletcher, and K. M. Thomas, *J. Am. Chem. Soc.*, 2008, **130**, 6411.